

## Diagnosing the AGN origin of diffuse TeV neutrinos with their spatial correlation

XIAO-BIN CHEN <sup>1,2</sup> RUO-YU LIU <sup>1,2,3</sup> AND XIANG-YU WANG <sup>1,2</sup>

<sup>1</sup>*School of Astronomy and Space Science, Nanjing University, Nanjing 210023, China*

<sup>2</sup>*Key laboratory of Modern Astronomy and Astrophysics (Nanjing University), Ministry of Education, Nanjing 210023, China*

<sup>3</sup>*Tianfu Cosmic Ray Research Center, Chengdu 610000, Sichuan, China*

### ABSTRACT

The recent detection of TeV neutrinos from some nearby Seyfert galaxy (e.g., NGC 1068) by IceCube suggests that active galactic nuclei (AGNs) could make a significant contribution to diffuse astrophysical neutrinos. The absence of TeV gamma-rays from NGC 1068 indicates neutrino production in a compact opaque region of gamma-rays. The vicinity of the supermassive black hole, such as the disk-corona, is an ideal region, where the high radiation density leads to efficient neutrino production and gamma-ray attenuation. Disk-corona models predict that the neutrino emission from AGNs correlates with X-ray emission, which traces the coronal activity. In this paper, we assess whether diffuse TeV neutrinos can originate from X-ray-emitting AGNs with Monte Carlo simulations, considering the predicted performance of future neutrino telescopes. We test this hypothesis by searching for spatial correlations between the X-ray AGN population and high-energy neutrinos, assuming that the neutrino flux scales with the AGN X-ray flux. Based on detailed Monte Carlo simulations, we find that an AGN origin of diffuse neutrinos can be tested at a significance of about  $3\sigma$  with five years of IceCube-Gen2 observations. With improved angular resolution and sensitivity, a 30 km<sup>3</sup>-scale underwater neutrino telescope (such as the High-energy Underwater Neutrino Telescope) is expected to reach a significance of about  $8\sigma$  with one year of exposure. The detection significance decreases if AGNs contribute partially to the total astrophysical neutrino flux. Our results highlight the critical role of angular resolution in diagnosing the AGN origin of diffuse TeV neutrinos.

*Keywords:* Neutrino astronomy (1100) — Active galactic nuclei (16)

### 1. INTRODUCTION

The IceCube neutrino telescope has detected a significant number of neutrinos with energies between a few TeV and a few PeV. Searches for point-like sources associated with known astrophysical objects have largely returned null detection (M. G. Aartsen et al. 2020a), suggesting that the high-energy neutrino sky is dominated by an isotropic background. Although the origins of the vast majority of high-energy neutrinos have not been identified, a significant excess coming from the close-by Seyfert galaxy NGC 1068 at  $4.2\sigma$  level (IceCube Collaboration et al. 2022) has been reported recently. Tentative excesses at  $3\sigma$  level have also been reported from some other NGC 1068-like AGNs such

as NGC 7469 and NGC 4151 (R. Abbasi et al. 2025a), implying that Seyfert galaxies could be the dominant sources of high-energy neutrinos.

The neutrino flux measured from NGC 1068 is more than an order of magnitude larger than the upper limits of TeV gamma-ray emission placed by MAGIC and HAWC (V. A. Acciari et al. 2019; E. Wilcox & HAWC Collaboration 2022). The difference between the observed neutrino flux and gamma-ray flux from NGC 1068 suggests that the neutrinos must be produced in a region that is opaque to GeV–TeV gamma-rays that would otherwise accompany the neutrinos. In Seyfert galaxies like NGC 1068, a hot and magnetized corona above the disk is formed (see e.g. K. A. Miller & J. M. Stone 2000). The dense environments near the supermassive black holes together with the acceleration of cosmic rays (CRs) in the corona offer suitable conditions for the production of high energy neutrinos. Such a scenario, commonly referred to as disk-corona mod-

els, has been shown to be able to accommodate the high level of neutrino emission from the X-ray bright AGN NGC 1068 (K. Murase et al. 2020; Y. Inoue et al. 2020; A. Kheirandish et al. 2021; B. Eichmann et al. 2022).

The large flux contrast between neutrinos and gamma rays in NGC 1068 is in agreement with the picture of gamma-ray “hidden” sources for the origin of the isotropic neutrino background (N. Senno et al. 2015; K. Murase et al. 2016; K. Bechtol et al. 2017; A. Capanema et al. 2020; K. Fang et al. 2022), as required by comparison of isotropic diffusive neutrino flux measured by IceCube (M. G. Aartsen et al. 2020b; R. Abbasi et al. 2022) and the isotropic gamma-ray background observed by Fermi-LAT (M. Ackermann et al. 2015). This consistency further supports the main contributors of the neutrino background are “hidden” sources. Building on this framework, D. F. G. Fiorillo et al. (2025) extended the NGC 1068 result to a population study of X-ray-emitting AGNs using the luminosity function of AGNs, showing that the cumulative neutrino emission from such sources can account for the diffuse neutrinos observed by IceCube in the 1-100 TeV energy range.

However, the limited angular resolution and statistics of current IceCube data make it difficult to establish a significant spatial correlation between neutrinos and the population of X-ray AGNs. Previous searches for spatial correlation have mainly relied on some classes of AGNs, such as blazars and radio-bright AGNs (e.g. B. Zhou et al. 2021; R. Abbasi et al. 2023, 2025b), but no significant excess has been found so far. Future neutrino telescopes, such as IceCube-Gen2 (M. G. Aartsen et al. 2021), KM3NeT (S. Adrián-Martínez et al. 2016), Huge Underwater high-energy Neutrino Telescope (HUNT) (T. Q. Huang et al. 2024), Tropical Deep-sea Neutrino Telescope (TRIDENT) (Z. P. Ye et al. 2023), NEON (H. Zhang et al. 2025) and Baikal-GVD (I. Belolaptikov et al. 2022), will have larger effective volumes and improved angular precision, and are therefore crucial for testing this correlation. Motivated by this, in this work, we assess whether the X-ray AGN origin for diffuse TeV neutrinos can be tested by using the spatial correlation between the X-ray AGN population and neutrino population with future neutrino telescopes. We will use IceCube-Gen2 and HUNT as two examples of future neutrino telescopes for the analyses. We assume the neutrino luminosity to be positively related to the X-ray luminosity of the AGN, given that the X-ray luminosity may reflect the energy production rate in the corona, and is also proportional to the target density for photopion production. By combining the AGN X-ray luminosity distribution with the expected performance of

future neutrino telescopes, we forecast the prospects for detecting such a AGN-neutrino correlation.

## 2. ANALYSIS TECHNIQUE

### 2.1. *Simulating Neutrino-AGN Associations*

We evaluate the spatial correlation between high-energy neutrinos and AGNs by comparing how well the observed neutrino directions agree with the expectations under two competing scenarios for their astrophysical origins:

1. **AGN Association Hypothesis:** A subset or all of the detected neutrinos originate from AGNs, with their flux scaling proportionally to the X-ray fluxes of AGNs. In this scenario, the X-ray flux of an AGN serves as the proxy for its neutrino flux, reflecting the case in which AGNs are genuine neutrino emitters.
2. **Null Hypothesis (Random Background):** Neutrino events are uncorrelated with AGNs and are isotropically distributed. Any apparent spatial association between AGNs and neutrinos arises purely by coincidence.

In both models, we account for contamination from atmospheric neutrinos, which form an irreducible background in high-energy neutrino observations. According to the IceCube 9.5-year dataset (R. Abbasi et al. 2022), the astrophysical signal starts to dominate the atmospheric neutrinos from 100 TeV. This motivates a further decomposition of the observed neutrino sample into its astrophysical and atmospheric components. We introduce the parameter  $\beta$ , defined as the fraction of astrophysical neutrinos relative to the total neutrino population (including atmospheric background) above a given energy threshold:

$$\beta(E_{\text{th}}) \equiv \frac{N_{\nu}^{\text{astro}}(E > E_{\nu}^{\text{th}})}{N_{\nu}^{\text{all}}(E > E_{\nu}^{\text{th}})}. \quad (1)$$

The value of  $\beta$  depends sensitively on the chosen neutrino energy threshold  $E_{\nu}^{\text{th}}$  and increases rapidly toward unity at higher energies, reflecting the diminishing contribution from atmospheric neutrinos. In this work,  $\beta(E_{\nu}^{\text{th}})$  is derived directly from IceCube observations (R. Abbasi et al. 2022) and is illustrated in Figure 1. In addition, we define the  $\alpha$  as the fraction of astrophysical neutrinos produced by AGNs:

$$\alpha \equiv \frac{N_{\nu}^{\text{AGN}}}{N_{\nu}^{\text{astro}}}, \quad (2)$$

which characterizes the efficiency of AGNs as neutrino sources relative to the total astrophysical neutrino flux.

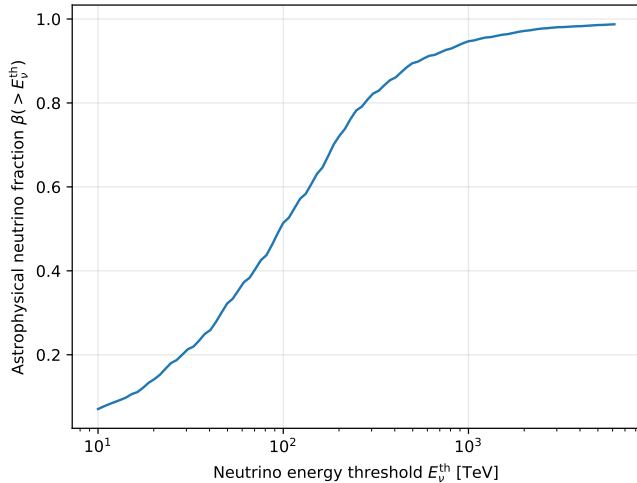


**Figure 1.** The fraction of astrophysical neutrinos  $\beta$  as a function of the neutrino energy threshold  $E_\nu^{\text{th}}$ , derived from IceCube observations (R. Abbasi et al. 2022). As the energy threshold increases, the atmospheric neutrino background is progressively suppressed, causing  $\beta$  to approach unity at high energies.

The AGN catalog from the eROSITA Final Equatorial-Depth Survey (eFEDS) (T. Liu et al. 2022) forms the basis of our analysis. It includes 22,079 AGNs selected by X-rays in a contiguous 142 deg<sup>2</sup> field, with fluxes measured in the 0.2 – 2.3 keV band. Given its depth ( $6.5 \times 10^{-15} \text{ erg s}^{-1} \text{ cm}^{-2}$ , H. Brunner et al. 2022) and well-characterized selection, the eFEDS sample provides a representative snapshot of the AGN population accessible to current wide-field X-ray surveys. Although eFEDS covers only a limited sky area, forthcoming all-sky and wide-area eROSITA AGN catalogs (e.g., M. Salvato et al. 2025) with comparable depth will substantially increase the AGN statistics and further enhance the sensitivity of our method.

Under the AGN-association hypothesis, we normalize the simulation by requiring that the total number of modeling neutrinos equals the expected number derived from the measured diffuse astrophysical neutrino flux plus the atmospheric neutrino background. These fluxes, taken from muon-neutrino flux with 9.5 years of IceCube data (R. Abbasi et al. 2022), are integrated over the chosen energy threshold and then folded with the effective area of the detector to yield the expected total count of events  $N_\nu^{\text{tot}}$ . The probability of each AGN producing a neutrino is taken to be proportional to its X-ray flux ( $F_X$ ), i.e.,  $P_i \propto F_{X,i}$ . The sum of all AGN population reproduces  $f_{\text{tot}} \cdot N_\nu^{\text{tot}}$ , in which the fraction  $f$  denotes the fraction of astrophysical neutrinos with energies above a given threshold relative to the total neutrino population. Because the AGN catalog is flux-limited,

the parameter  $f$  captures only the contribution from X-ray-bright AGNs. To estimate the total AGN population contribution, including X-ray-faint AGNs below the threshold  $F_{\text{min}}$ , we extrapolate using the AGN X-ray luminosity function. The total AGN neutrino fraction is then given by

$$f_{\text{tot}} = f \cdot \frac{\sum_{\text{all}} F_X}{\sum_{F_X > F_{\text{min}}} F_X}, \quad (3)$$

and the expected value of this quantity is  $\alpha \times \beta$ .

For each AGN-origin neutrino assigned, its arrival direction is offset from the source position according to a two-dimensional Gaussian with a width equal to the detector’s point-spread function (PSF). In contrast, under the null hypothesis, neutrino positions are randomly drawn from a uniform distribution across the same sky footprint, with no relation with AGN locations.

## 2.2. Unbinned Likelihood Framework for Spatial Correlation Analysis

An unbinned likelihood ratio method can be used to distinguish astrophysical neutrinos from the atmospheric background produced by cosmic ray interactions (J. Braun et al. 2008; C. Creque-Sarbinowski et al. 2022; R. Abbasi et al. 2024). The analysis is designed to measure the fractional contribution of AGN-generated neutrinos to the all-sky neutrino sample. The optimal estimator to determine the fraction  $f$  of neutrinos associated with AGN is obtained using the unbinned maximum likelihood (ML) approach, formulated as

$$\mathcal{L}(f) = \prod_{i=1}^N [f \cdot S_i + (1 - f) \cdot B_i], \quad (4)$$

where  $S_i$  and  $B_i$  represent the signal and background probability density functions (PDFs), respectively, for the  $i$ -th neutrino event. The signal PDF  $S_i$  represents the likelihood of the  $i$ -th neutrino originating from the AGN population, modeled as a weighted sum over all AGNs in the field:

$$S_i = \sum_j w_j \frac{1}{2\pi\sigma_{\text{psf}}^2} \exp\left(-\frac{(\vec{x}_i - \vec{x}_j)^2}{2\sigma_{\text{psf}}^2}\right), \quad (5)$$

where  $\vec{x}_i$  and  $\vec{x}_j$  are the reconstructed positions of the neutrino and the  $j$ -th AGN, respectively, and  $w_j = F_j / \sum_k F_k$  reflects the X-ray flux-weighted contribution of each AGN. Here  $F_j$  denotes the observed X-ray flux of the  $j$ -th AGN in the 0.2–2.3 keV band, as reported in the eFEDS catalog. The parameter  $\sigma_{\text{psf}}$  characterizes the angular resolution (i.e. PSF) of the neutrino detector. The background PDF  $B_i$  accounts for neutrinos

arising from the isotropic atmospheric background and is modeled as a uniform distribution over the analysis region:  $B_i = \frac{1}{\Omega}$ , where  $\Omega$  is the solid angle subtended by the sky region covered by the AGN catalog and neutrinos.

The signal fraction  $f$  is determined by maximizing the likelihood function  $\mathcal{L}(f)$  constructed over all observed neutrino events. Under the null hypothesis (i.e., no AGN contribution), the likelihood reduces to  $\mathcal{L}(f = 0) = \prod_{i=1}^N B_i$ . The strength of the signal is then quantified by the likelihood ratio test statistic:

$$\text{TS} = \lambda = -2 \cdot \log \left[ \frac{\mathcal{L}(f)}{\mathcal{L}(f = 0)} \right], \quad (6)$$

which measures the relative preference for a nonzero  $f$  over the null hypothesis. In the large-sample limit, TS approximately follows a  $\chi^2$  distribution with one degree of freedom, and the statistical significance can be estimated as  $\sigma \simeq \sqrt{\text{TS}}$ . The validity of this approximation has been verified with  $5 \times 10^6$  background-only Monte Carlo simulations (see Appendix A). Finally, we note that the total AGN neutrino fraction inferred from the likelihood analysis,  $f_{\text{tot}}$ , admits a simple physical interpretation.

To quantify the uncertainty on the total AGN neutrino fraction, we define the relative error  $\delta$ :

$$\delta \equiv \delta_{f_{\text{tot}}} = \frac{\sigma_{f_{\text{tot}}}}{f_{\text{tot}}}, \quad (7)$$

where  $\sigma_{f_{\text{tot}}}$  is obtained from the distribution of  $f_{\text{tot}}$  over 800 independent Monte Carlo realizations, and therefore includes both statistical fluctuations (i.e., the Poisson fluctuations in the expected number of neutrino events) and systematic uncertainties, which will be discussed in Section 4.

### 2.3. Mitigating Source Confusion in Analyses

Likelihood-based methods provide a powerful statistical framework for estimating the neutrino signal fraction  $f_{\text{tot}}$ . However, it does not sufficiently address the impact of source confusion—a fundamental limitation in astronomical surveys that arises when the instrument’s angular resolution is too coarse to distinguish nearby sources (X. Barcons 1992; P. Kurczynski & E. Gawiser 2010; M. G. Jones et al. 2016). As also noted by M. Kowalski et al. (2025), stacking becomes unreliable when the average number of sources within a single PSF exceeds one, resulting in systematic underestimate of  $f_{\text{tot}}$ .

To quantify this effect, we investigate how the mean angular separation between sources ( $\bar{d}$ ) interacts with the detector’s PSF width ( $\sigma_{\text{psf}}$ ). Since brighter sources tend to be more sparsely distributed, adjusting  $F_{\text{min}}$

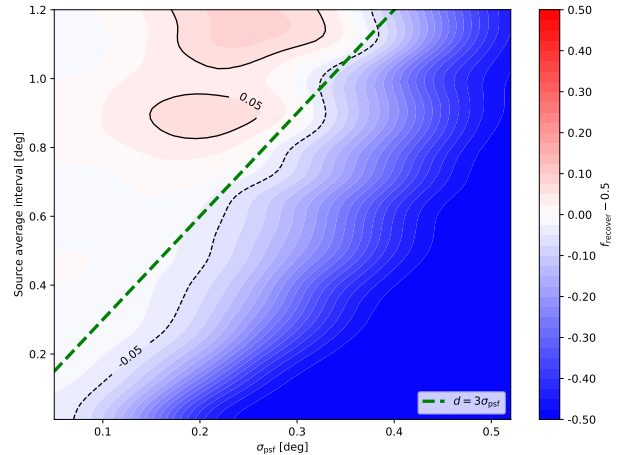


**Figure 2.** Deviation of the recovered signal fraction from the true value,  $f_{\text{tot}} - 0.5$ , as a function of PSF and average source separation. Red (blue) regions indicate positive (negative) deviations, while the white region corresponds to no bias (i.e.,  $f_{\text{tot}} = 0.5$ ). The green dashed line marks  $d = 3\sigma_{\text{psf}}$ , above which the recovered fraction converges to the true value  $f_{\text{tot}} = 0.5$ .

provides a practical way to control the source density. Specifically, we define a minimum separation  $d$  and determine the corresponding  $F_{\text{min}}$  such that the selected AGNs have a typical spacing larger than  $\bar{d}$ . This approach allows us to explore a wide range of source densities while maintaining physical realism.

Figure 2 summarizes the results for a fixed true value  $f_{\text{tot}} = 0.5$ . When the average separation satisfies  $\bar{d} \geq 3\sigma_{\text{psf}}$ , the maximum-likelihood estimator reliably recovers the true  $f$ . In contrast, for denser source populations ( $\bar{d} \leq 3\sigma_{\text{psf}}$ ), confusion effects cause  $f$  to be systematically underestimated. We note that the present analysis is based on the eFEDS AGN catalog, which covers a relatively limited sky area of  $142 \text{ deg}^2$ . In regimes where the source density is low and the average separation becomes large, the finite survey area can amplify statistical fluctuations, resulting in increased scatter in the recovered  $f_{\text{tot}}$ , as visible in the upper-left region of Figure 2. This effect is primarily driven by limited source statistics rather than a failure of the likelihood method itself. In future wide-area X-ray surveys with substantially larger sky coverage, this statistical limitation will be significantly alleviated, leading to more stable and accurate parameter recovery. This yields a practical condition for method applicability: the source population must be sufficiently sparse, such that the average spacing between sources exceeds approximately three times the PSF width. Importantly, we verify that this trend is valid for a wide range of values of  $f_{\text{tot}}$ , not just for the specific case of  $f_{\text{tot}} = 0.5$ . In the following analyses,

this empirical requirement,  $\bar{d} \geq 3\sigma_{\text{psf}}$ , is adopted as a baseline condition to ensure that source confusion does not bias the likelihood inference.

Based on this empirical criterion, we set a minimum X-ray flux threshold  $F_{\text{min}}$  for all subsequent analyses, such that the selected AGN subset satisfies  $\bar{d} \geq 3\sigma_{\text{psf}}$ . Since more luminous AGNs are more sparsely distributed on the sky, adjusting  $F_{\text{min}}$  provides a practical way to control the source density and to ensure that the selected population remains well resolved. This choice mitigates confusion-induced bias and preserves the validity of the maximum-likelihood inference. The resulting sample therefore represents only the relatively bright portion of the full AGN population. All reported values of  $f_{\text{tot}}$  in this work, including those shown in Figure 2, incorporate this correction, ensuring consistency with the full AGN population even though the likelihood analysis itself is restricted to the bright subset.

### 3. PREDICTIVE POWER FOR FUTURE NEUTRINO DETECTORS

Next-generation neutrino observatories are expected to greatly enhance the capability to detect astrophysical neutrino sources. Proposed facilities such as IceCube-Gen2, HUNT, TRIDENT, NEON and Baikal-GVD, also promise enhanced exposure and angular resolution. These advances motivate us to examine how the improvements in angular resolution, event statistics, and energy threshold affect the prospects for diagnosing the neutrino–AGN correlation.

In this section, we consider a special scenario in which all astrophysical neutrinos originate from AGNs, corresponding to  $\alpha = 1$ . This idealized case represents the maximal AGN contribution to the diffuse astrophysical neutrino flux and provides an upper limit on the expected signal in future detectors. Studying this scenario allows us to explore the full potential of next-generation instruments to constrain or detect neutrino–AGN associations under optimal conditions.

We perform a series of simulations to quantify how key observational parameters influence the detection potential. Specifically, we examine four primary factors: the detector’s angular resolution, the total number of detected neutrinos, the minimum energy threshold, and the observation duration. These variables determine both the statistical power and the level of background contamination, which jointly govern the overall sensitivity of correlation searches.

Figure 3 illustrates how the detection significance depends on the angular resolution and the total number of detected neutrinos, where the astrophysical neutrino fraction above 100 TeV is fixed at  $f = 0.5$ , consistent

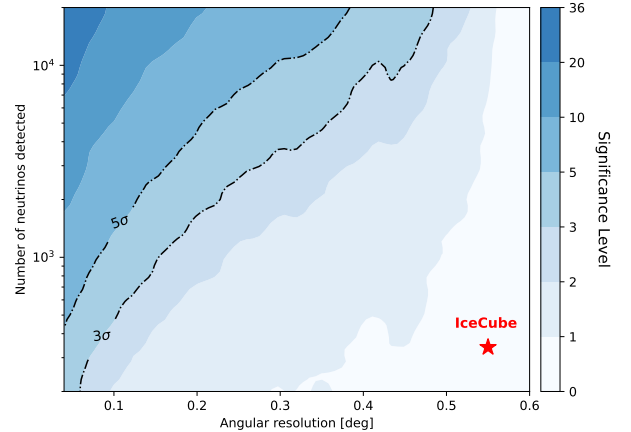


**Figure 3.** Detection significance as a function of angular resolution and the total number of detected neutrinos. The color map indicates the significance level, with solid and dashed contours marking the  $5\sigma$  and  $3\sigma$  confidence levels, respectively. The gold star denotes the parameter point corresponding to the *IceCube Alert* event (A. Zegarelli et al. 2025).

with the IceCube measurements. (R. Abbasi et al. 2022) The trends are clear: improving the angular resolution reduces positional uncertainties, thereby increasing the contrast between AGN–neutrino associations and random coincidences. At a fixed angular resolution, increasing the total event count enhances the statistical weight of the likelihood, roughly following the expected  $(S/N)_f \propto \sqrt{N}$  scaling. On the other hand, for a fixed number of detected neutrinos, the significance decreases with increasing PSF width by  $(S/N)_f \propto \sigma_{\text{psf}}^{-1}$ . Notably, achieving a  $5\sigma$  detection requires only  $\sim 2000$  events for an angular resolution of  $0.1^\circ$ , whereas resolution worse than  $0.4^\circ$  demands at least two orders of magnitude more events, making identification of the correlation unattainable. As marked with the red star in Figure 3, with  $\sim 10^2$ – $10^3$  detected astrophysical neutrinos and a median angular uncertainty of  $\sim 0.55^\circ$  above 100 TeV (A. Zegarelli et al. 2025), IceCube’s observations do not have sufficient exposure and angular resolution to diagnosing the AGN origin of diffuse TeV neutrinos: the current IceCube data lies far below the regime where AGN population correlations could be statistically established (denoted by “IceCube” in Figure 3). This highlights the importance of angular resolution. This trend can be understood as the combined result of two complementary effects acting at different levels of the analysis. First, at the population level, a smaller  $\sigma_{\text{psf}}$  mitigates source confusion and allows the likelihood analysis to incorporate contributions from a larger fraction of the AGN population, including sources with weaker X-ray emission, provided that the mean source

separation satisfies  $\bar{d} \geq 3\sigma_{\text{psf}}$ . In this regime, reducing  $\sigma_{\text{psf}}$  allows more sources to satisfy  $\bar{d} \geq 3\sigma_{\text{psf}}$ , so that they can be included in the likelihood with non-negligible weights (the  $w_j$  of Eq. 5), thereby enhancing the cumulative statistical power. Second, at the event level, improved angular resolution sharpens the spatial probability density of each neutrino event, concentrating the signal likelihood around the true source positions. This reduces the overlap with the isotropic background term and increases the contrast between genuine AGN–neutrino associations and random coincidences (i.e., the  $S_i$  and  $B_i$  of Eq. 4), leading to a larger likelihood ratio and a higher detection significance.

Building upon the angular resolution-based considerations described above, we next examine how the selection of different neutrino energy bands influences the source identification capabilities. In particular, the fraction of detected neutrino events above a given energy threshold plays a key role in the achievable detection significance: astrophysical neutrinos from AGN are expected to dominate at higher energies, while the atmospheric background falls steeply. Moreover, higher-energy neutrinos are reconstructed with better angular resolution, further enhancing source identification capabilities.

Figure 4 illustrates the trade-off between neutrino energy threshold and exposure time for future neutrino observatories, with the left panel corresponding to IceCube-Gen2 and the right panel to the proposed HUNT detector. The horizontal axis denotes the minimum reconstructed neutrino energy threshold applied to the event sample, while the vertical axis indicates the observation time. For IceCube-Gen2, we adopt an energy-dependent angular resolution based on muon track reconstruction reported in [F. Bradascio & T. Glüsenskamp \(2019\)](#), together with the corresponding effective area taken from the official IceCube-Gen2 design study ([M. G. Aartsen et al. 2021](#)). For the HUNT detector, the calculation incorporates its energy-dependent angular resolution and effective area from the simulations ([T. Q. Huang & HUNT Collaboration 2025](#)).

As the energy threshold of neutrinos increases, two competing effects emerge: (i) the angular resolution improves and the atmospheric neutrino flux drops; (ii) the number of neutrino events above the energy threshold declines, reducing statistical power. These opposing trends jointly define an optimal energy window, typically around a few hundred TeV, where the sensitivity peaks (100 TeV for IceCube-Gen2 and 300 TeV for HUNT). Beyond this regime, further increases in the energy threshold result in diminishing returns due to limited event statistics.

Within the same physical framework, the superior performance of the HUNT detector can be understood in terms of its expected design characteristics. Based on its projected, energy-dependent performance, HUNT is anticipated to achieve a median angular resolution that is improved by a factor of  $\sim 4\text{--}5$  relative to IceCube-Gen2, together with an effective area larger by a factor of  $\sim 3$  in the relevant energy range (a few hundred TeV). These factors summarize the relative detector performance inferred from their respective design specifications, rather than representing a direct rescaling of IceCube-Gen2 parameters. As a result, HUNT attains a higher detection significance—or equivalently, requires a shorter exposure time—for a given neutrino energy threshold.

#### 4. IMPACT OF SYSTEMATIC AND POSITIONAL UNCERTAINTIES

The analyses presented thus far have assumed idealized conditions: the AGN X-ray luminosity function (XLF) was treated as perfectly known, and the neutrino angular uncertainty was assumed to be fixed for all events. In practice, both of them have uncertainties, so they could introduce additional uncertainties in the inferred signal fraction  $f_{\text{tot}}$ . Here we quantify the contributions from these two dominant sources of uncertainty and evaluate their combined impact on the overall detection significance. In addition to these systematic effects, statistical fluctuations due to the finite neutrino sample are automatically incorporated in all Monte Carlo realizations, and are not treated as a separate source of uncertainty. As the exposure increases, the impact of these statistical fluctuations diminishes, and the total uncertainty becomes increasingly dominated by systematic effects.

The first source of the systematic uncertainty arises from extrapolating the neutrino contribution inferred from the bright, flux-limited AGN subset ( $F_X > F_{\text{min}}$ ) to the full AGN population. In our baseline analysis, this extrapolation is implemented using the observed X-ray flux distribution of the eFEDS AGN catalog, which provides a data-driven correction without assuming a specific parametric form. However, the eFEDS sample does not fully represent the global AGN population, particularly toward low luminosities and high redshifts, where the bulk of the luminosity density resides.

To quantify the systematic uncertainty associated with this extrapolation, we alternatively model the AGN population using a parametric XLF. Assuming that the neutrino luminosity scales linearly with the X-ray luminosity (e.g., [R. Abbasi et al. 2022](#); [E. Kun et al. 2024](#)), the total neutrino flux can be written as

$$\Phi_{\nu}^{\text{tot}} \propto \int_{L_{\text{min}}}^{L_{\text{max}}} L_X \phi(L_X, z) dL_X dz, \quad (8)$$

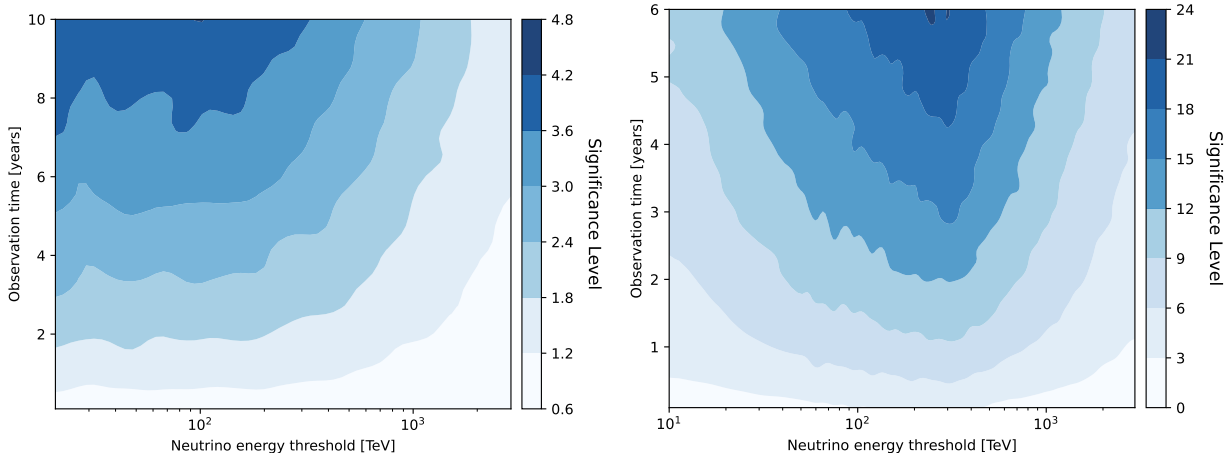


**Figure 4.** Trade-off between neutrino energy threshold and exposure time for future neutrino observatories. **The left panel** shows results for IceCube-Gen2, adopting the projected energy-dependent angular resolution from [F. Bradascio & T. Glüsenskamp \(2019\)](#). **The right panel** shows the corresponding results for the proposed 30 km<sup>3</sup> HUNT detector, incorporating its energy-dependent angular resolution and effective area from [T. Q. Huang & HUNT Collaboration \(2025\)](#).

where  $\phi(L_X, z)$  denotes the XLF.

Using the best-fit XLF parameters and their reported  $1\sigma$  uncertainties from [Y. Ueda et al. \(2014\)](#), we perform Monte Carlo simulations in which the XLF parameters are randomly varied according to independent Gaussian distributions centered on their best-fit values. For each realization, we compute the corresponding correction factor between the flux-limited subset and the full population, thereby estimating the relative uncertainty of the extrapolated neutrino contribution as a function of the adopted flux threshold  $F_{\min}$ . That quantifies the relative uncertainty in the extrapolated total AGN neutrino contribution induced solely by XLF uncertainties, which we denote as  $\delta_{\text{XLF}}$ . The resulting  $\delta_{\text{XLF}}$  as a function of  $F_{\min}$  is summarized in Figure 5. As expected, adopting brighter flux thresholds leads to rapidly increasing extrapolation uncertainties. This behavior reflects the fact that when only very luminous AGNs are included, the selected subset captures only a small fraction of the total XLF-weighted luminosity density, causing the correction factor to become highly sensitive to uncertainties in the faint-end slope and normalization of the XLF.

As discussed in [Sec. 2.2](#), the total AGN neutrino fraction  $f_{\text{tot}}$  is obtained by applying a flux-based extrapolation to the flux-limited likelihood result, as defined in [Eq. \(3\)](#). Uncertainties in the XLF-based extrapolation propagate directly into the inferred total AGN neutrino fraction  $f_{\text{tot}}$ . In the Monte Carlo framework, this appears as a broadening of the reconstructed  $f_{\text{tot}}$  distribution, characterized by an increased standard deviation  $\sigma_{f_{\text{tot}}}$ , while the mean remains approximately unbiased. We quantify the impact of this effect using the relative uncertainty  $\delta$ . When  $\delta > 50\%$ , the inference of  $f_{\text{tot}}$  becomes dominated by XLF systematic uncertainty rather

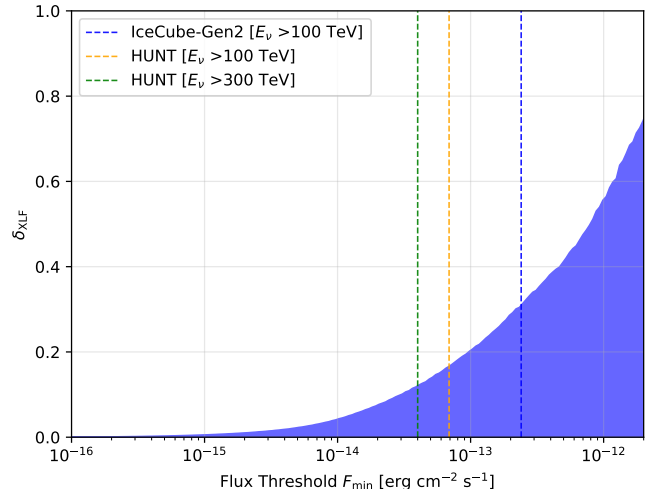


**Figure 5.** Relative uncertainty factor  $\delta_{\text{XLF}}$  of XLF in the extrapolated AGN contribution as a function of the AGN flux threshold  $F_{\min}$ . The shaded band shows the 68% confidence interval derived from Monte Carlo realizations. The vertical blue, orange, and green lines mark the values of  $F_{\min}$  adopted for IceCube-Gen2 ( $E_\nu > 100$  TeV), HUNT ( $E_\nu > 100$  TeV), and HUNT ( $E_\nu > 300$  TeV), respectively. Uncertainties remain modest at low thresholds but grow rapidly when only the brightest AGNs are included.

than statistical fluctuations, and the extrapolated AGN contribution is no longer robustly constrained. To avoid this regime, we restrict our analysis to flux thresholds  $F_{\min} < 7 \times 10^{-13}$  erg cm<sup>-2</sup> s<sup>-1</sup>, which corresponds to the stability criterion quantified above, as shown in [Figure 5](#). In this range, the selected AGN subset encompasses a substantial fraction of the total XLF-weighted luminosity density, and the extrapolation remains stable against variations in the XLF parameters.

The second uncertainty arises from the event-by-event variations in the  $\sigma_{\text{psf}}$ . In previous sections, we adopted a fixed PSF width  $\sigma_{\text{psf}}$  for given energy bins, whereas real detectors exhibit a distribution of reconstructed angular uncertainties. This variation effectively broadens the signal and background probability density functions used in the maximum-likelihood analysis, thereby reducing sensitivity. To quantify this effect, we simulate neutrino samples by assigning to each event a  $\sigma_{\text{psf}}$  randomly sampled from the detector’s energy-dependent angular resolution distribution. We find that the uncertainty induced by event-by-event PSF variations is smaller than that from the XLF-based extrapolation, and therefore does not dominate the total error budget.

Combining the uncertainties from both XLF extrapolation and PSF variation, we assess the sensitivity of future neutrino telescopes to testing the AGN-origin hypothesis. In the simulations, the angular uncertainty of each neutrino event is treated on an event-by-event basis, with the reconstructed direction randomly drawn according to the corresponding point-spread function, thereby accounting for realistic variations in the localization accuracy. Focusing on events with energies above 100 TeV ( $\beta \simeq 0.5$ ), IceCube-Gen2 is expected to achieve a median angular resolution of  $\sim 0.2^\circ$ . To avoid source confusion, we therefore require the selected AGN population to satisfy the condition  $\bar{d} \geq 0.6^\circ$ . Based on the eFEDS AGN catalog over the  $142 \text{ deg}^2$  survey area, this requirement translates into a maximum of  $\sim 150$  AGNs within the field of view. This criterion selects the brightest sources with X-ray fluxes  $F_X > 2.4 \times 10^{-13} \text{ erg s}^{-1} \text{ cm}^{-2}$ , which are sufficiently sparse to remain well resolved at the IceCube-Gen2 angular resolution. As shown in Figure 5, for the flux threshold corresponding to IceCube-Gen2 (blue vertical line), the uncertainty induced by the XLF-based extrapolation from the flux-limited AGN subsample to the full AGN population is  $\delta_{\text{XLF}} \simeq 30\%$ . As shown in Figure 6, such the detector would achieve a significance of approximately  $\sim 3.1\sigma$  after five years of exposure in testing whether all astrophysical neutrinos originate from AGN population. This significance is suggestive but insufficient for a decisive test of the AGN-origin hypothesis.

As an illustrative and more optimistic case, we consider the HUNT, a proposed  $30 \text{ km}^3$  underwater neutrino detector (T. Q. Huang et al. 2024; T. Q. Huang & HUNT Collaboration 2025) and focus on events with energies above 300 TeV ( $\beta \simeq 0.8$ ), for which an angular resolution of  $\sim 0.04^\circ$  is expected at these energies. At this energy threshold, we restrict the analysis to AGNs with X-ray fluxes  $F_X > 4 \times 10^{-14} \text{ erg s}^{-1} \text{ cm}^{-2}$ . Based on the eFEDS AGN catalog, this  $\bar{d} \geq 3\sigma_{\text{psf}}$  condition

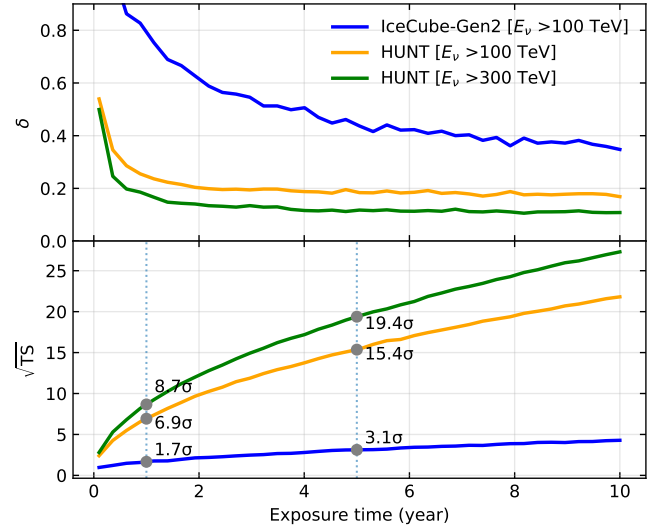


**Figure 6.** **Top panel:** Relative uncertainty on the inferred total AGN neutrino fraction  $\delta$  as a function of the exposure time, derived from repeated Monte Carlo simulations. **Bottom panel:** The detection significance, expressed as  $\sqrt{TS}$ , as a function of exposure time. The steady decrease of  $\delta$  and the growth of  $\sqrt{TS}$  demonstrate how both the precision and statistical significance of the AGN contribution improve with increased exposure.

corresponds to a maximum surface density of  $\sim 3200$  sources, which in turn selects the brightest AGNs with  $F_X > 4 \times 10^{-14} \text{ erg s}^{-1} \text{ cm}^{-2}$ . Such a relatively low flux threshold significantly reduces the uncertainty associated with the XLF-based extrapolation. As indicated by the green vertical line in Figure 5, the corresponding relative uncertainty is  $\delta_{\text{XLF}} \simeq 10\%$ . We find that HUNT can test the AGN-origin hypothesis at a confidence level of roughly  $8.7\sigma$  after one years of exposure, after accounting for uncertainties from both XLF extrapolation and PSF variation, as shown in Figure 6. At the same time, the likelihood analysis constrains the total AGN neutrino fraction to a relative precision of  $\delta \simeq 20\%$ . With five years of exposure, the significance further increases to  $\sim 19\sigma$ , and the relative uncertainty decreases to  $\delta \simeq 10\%$ .

For comparison, we also consider a more conservative energy threshold of  $E_\nu > 100 \text{ TeV}$  for HUNT. In this case, the larger angular uncertainty requires a brighter AGN flux threshold (orange vertical line in Figure 5), leading to a larger XLF extrapolation uncertainty and consequently a lower detection significance (orange curve in Figure 6), although the AGN-origin hypothesis remains testable at high confidence with multi-year exposure.

## 5. DISCUSSION

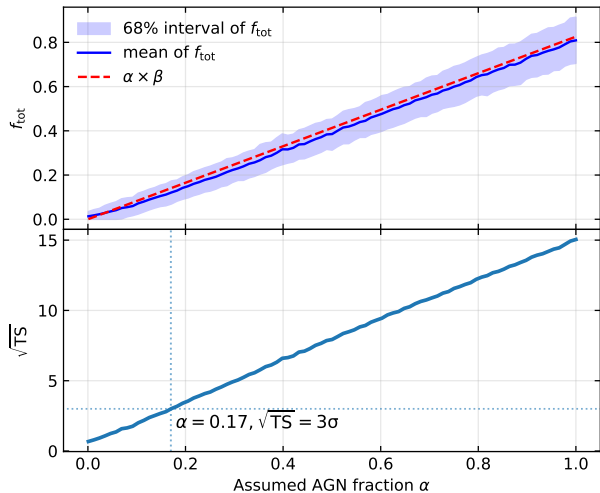


**Figure 7.** **Top panel:** Recovered AGN neutrino fraction  $f_{\text{tot}}$  as a function of the assumed AGN neutrino fraction  $\alpha$ . The blue shaded band shows the central 68% interval from 800 Monte Carlo realizations, while the solid blue line indicates the mean of  $f_{\text{tot}}$  from the simulations. The red dashed line represents the theoretical expectation  $f_{\text{tot}} = \alpha \times \beta$ , showing good agreement between the likelihood reconstruction and the expected value. **Bottom panel:** Corresponding detection significance  $\sqrt{\text{TS}}$  as a function of  $f_{\text{tot}}$ , showing that even partial AGN contributions can be detected with high statistical significance.

### 5.1. AGNs contributing partially to the total astrophysical neutrino flux

Throughout most of this work we have assumed the limiting case in which AGNs are assumed to be the dominant contributors to the observed astrophysical neutrino flux. In reality, the diffuse neutrinos could be produced by a mixture of source populations, and AGNs may account for only a fraction of the total astrophysical neutrino flux. Our framework readily accommodates this more general scenario: the parameter  $f_{\text{tot}}$  in the unbinned maximum-likelihood formalism already represents the fraction of events associated with AGNs, while the remaining  $(1 - f_{\text{tot}})$  fraction is treated as isotropic background.

Figure 7 demonstrates how the detection significance  $\sqrt{\text{TS}}$  scales with  $f_{\text{tot}}$  for a representative next-generation detector scenario (a  $30 \text{ km}^3$ -scale underwater neutrino telescope with 3 years of exposure). The top panel shows the recovered total AGN neutrino fraction  $f_{\text{tot}}$ , obtained from repeated Monte Carlo simulations, as a function of the assumed AGN neutrino fraction  $\alpha$ . The shaded region reflects the  $1\sigma$  uncertainty from the simulations, demonstrating that the likelihood analysis provides an unbiased reconstruction of  $f_{\text{tot}}$  across a wide range of AGN contributions. The

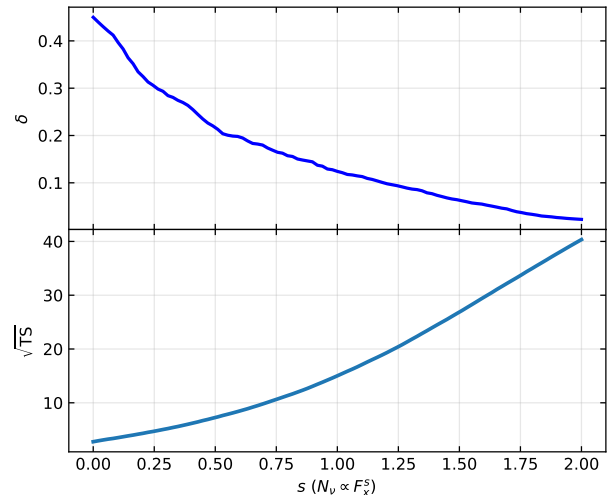


**Figure 8.** **Top panel:** Relative uncertainty of the recovered AGN neutrino fraction  $\delta$  as a function of the flux-weighting parameter  $s$  ( $N_\nu \propto F_X^s$ ). **Bottom panel:** Detection significance  $\sqrt{\text{TS}}$  as a function of the flux-weighting parameter  $s$ , illustrating that stronger weighting toward luminous AGNs enhances the detectability. All panels correspond to a  $30 \text{ km}^3$  undersea neutrino telescope with 3 years of exposure.

solid line shows the mean recovered  $f_{\text{tot}}$  from the simulations, which agrees well with the theoretical expectation  $f_{\text{tot}} \simeq \alpha \times \beta$ . The bottom panel displays the corresponding detection significance, expressed as  $\sqrt{\text{TS}}$ , as a function of  $\alpha$ . A vertical marker indicates the value  $\alpha \simeq 0.17$ , where  $\sqrt{\text{TS}} = 3$ . This highlights that if AGNs contribute less than  $\sim 17\%$  of the total astrophysical neutrino flux, the 3-year HUNT exposure would be insufficient to achieve a  $3\sigma$  detection. We further verify that even with an extended exposure of 10 years, AGN contributions below  $\alpha \simeq 0.09$  remain undetectable at the  $3\sigma$  level (i.e.,  $\sqrt{\text{TS}} < 3$ ). For larger AGN contributions,  $\sqrt{\text{TS}}$  scales approximately linearly with  $f_{\text{tot}}$ , reflecting the fact that the likelihood analysis primarily probes the spatially correlated AGN component, while the total uncertainty remains dominated by the isotropic background and the systematic uncertainties associated with the XLF-based extrapolation.

### 5.2. X-ray flux-weighting

So far, we have assumed a linear relationship between the number of neutrinos and the AGN X-ray flux. This treatment considers that the X-ray flux of an AGN may be a proxy for its high-energy proton power and also representative for the target density for neutrino production. However, the linear relationship is unwarranted yet (e.g., A. Ambrosone 2024; L. Saurenhaus et al. 2025). To generalize this idea, we explore a family of models

in which the neutrino flux from an AGN scales with its X-ray flux as  $N_\nu \propto F_X^s$ . The parameter  $s$  reflects the assumed physical correlation strength:  $s = 0$  corresponds to no dependence (i.e., uniform weighting across AGNs), while increasing  $s$  emphasizes the role of brighter AGNs in neutrino production. In this case, the source weights in Equation 5 of the likelihood function are modified to  $w_j = F_j^s / \sum_k F_k^s$  ensuring that the simulated neutrino–AGN associations reflect the chosen correlation index  $s$ .

We also consider a special scenario in which all astrophysical neutrinos originate from AGNs, corresponding to  $\alpha = 1$ . Figure 8 summarizes the impact of the flux-weighting parameter  $s$  on both the precision of the recovered AGN neutrino fraction and the overall detection significance, for a  $30 \text{ km}^3$  neutrino telescope with three years of exposure. The top panel of Figure 8 displays the relative uncertainty of the recovered AGN neutrino fraction  $\delta$ . We find that  $\delta$  decreases monotonically with increasing  $s$ , indicating that the precision of the recovered AGN contribution improves as neutrino emission becomes more strongly associated with X-ray–bright sources. The bottom panel shows the detection significance, quantified by  $\sqrt{\text{TS}}$ , as a function of  $s$ . A clear monotonic increase is observed, indicating that stronger weighting toward luminous AGNs substantially enhances the detectability of the population-level correlation. In the limit  $s \simeq 0$ , corresponding to uniform source weighting, the detection significance remains modest, at the level of  $\sim 2\sigma$ . As  $s$  approaches unity, implying a near-linear proportionality between neutrino and X-ray flux, the significance improves markedly, reflecting the growing dominance of the brightest AGNs in the signal. This behavior can be understood as a consequence of two related effects. First, larger values of  $s$  effectively suppress the contribution from faint AGNs while simultaneously increasing the relative weight of X-ray–bright sources, which significantly enhances the detection significance and reduces the statistical uncertainty in the recovered AGN neutrino fraction. Second, smaller values of  $s$  assign a relatively larger weight to faint AGNs, for which the extrapolation of the XLF introduces substantial systematic uncertainties, further inflating the uncertainty in the recovered fraction.

Overall, these results suggest that if astrophysical neutrino production preferentially traces the most luminous AGNs, both the detectability of the AGN–neutrino correlation and the precision of the inferred AGN neutrino fraction are significantly improved. Conversely, weaker flux weighting ( $s < 0.5$ ) implies a larger relative contribution from faint AGNs, leading to reduced signal

contrast with respect to the isotropic background and increased uncertainty in the recovered fraction.

### 5.3. Blazars Neutrino Predictions

Blazars are also widely discussed as possible sources of extragalactic neutrinos, and are likely to contribute a significant fraction in the diffuse neutrino intensity at sub-PeV energies (e.g., K. Murase et al. 2014; IceCube Collaboration et al. 2018; S. Das et al. 2022; S. Buson et al. 2022). Motivated by the association of TXS 0506+056 with a hard-spectrum ( $\Gamma \approx 2$ ) neutrino flare, we focus on the contribution of blazars to neutrinos above  $\sim 100 \text{ TeV}$ , where such sources are expected to be more prominent.

To directly test this scenario, IceCube has performed dedicated searches for cumulative emission from GeV–selected blazar populations (M. G. Aartsen et al. 2017). No significant excess was observed, and the upper limits constrain the contribution of 2LAC blazars to  $\lesssim 27\%$  of the observed diffuse neutrino flux between 10 TeV and 2 PeV (for a spectral index  $\Gamma = 2.5$ ). Nevertheless, it is reasonable to expect that their relative contribution becomes more significant above  $\sim 100 \text{ TeV}$ , and hence we focus on this higher-energy regime to assess the role of blazars as neutrino sources.

We consider 3933 blazars from the fourth Fermi-LAT catalog (J. Ballet et al. 2023), which provide a representative sample for our study. We also extrapolate their collective neutrino contribution using the GeV gamma-ray luminosity function (GLF) (S. Manconi et al. 2020), following the same procedure as that applied to the AGN XLF in Section 4. The left panel of Figure 9 presents the cumulative fraction of the total blazar neutrino flux as a function of flux threshold, with shaded regions showing the 68% and 95% credible intervals. Here, the “flux threshold” corresponds to the average energy flux detection limit of Fermi-LAT, representing the approximate completeness threshold of the blazar sample. Given that the mean sensitivity limit for the Fermi-LAT blazar sample is about  $2 \times 10^{-12} \text{ erg s}^{-1} \text{ cm}^{-2}$  (M. Ajello et al. 2022), we estimate that this Fermi-LAT blazar population accounts for approximately  $\sim 85\% \pm 5\%$  of the total neutrino emission from all blazars. This result is broadly consistent with previous Fermi-LAT studies of the blazar population at high energies. In particular, analyses of the extragalactic  $\gamma$ -ray background above  $\sim 50 \text{ GeV}$  have shown that the bulk of the total  $\gamma$ -ray energy density is dominated by resolved blazars, while the contribution from unresolved, low-flux sources is subdominant (e.g., M. Ackermann et al. 2016). Similar conclusions have been reached through stacking analyses of faint and extreme blazar populations, which in-

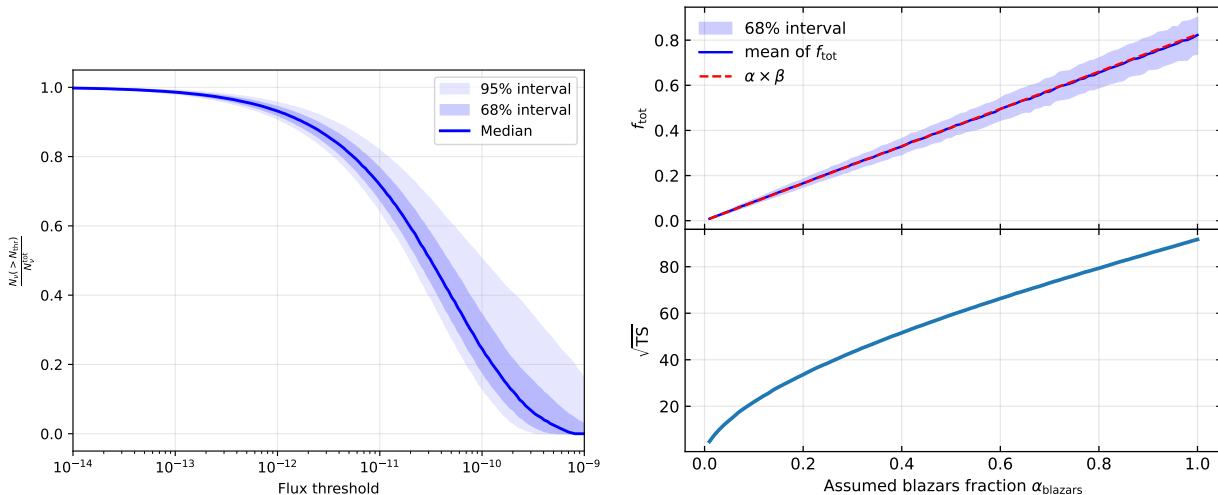


**Figure 9.** **Left:** Cumulative fraction of the total neutrinos contributed by blazars as a function of the gamma-ray flux threshold of blazars. The solid line shows the median, while the shaded regions indicate the 68% and 95 % credible intervals. **Right:** Top panel: Same as the Figure 7, recovered blazar neutrinos fraction  $f_{\text{tot}}$  as a function of the blazar neutrino fraction  $\alpha_{\text{blazars}}$ . Bottom panel: Corresponding detection significance  $\sqrt{\text{TS}}$  as a function of  $\alpha_{\text{blazars}}$ , showing that even partial blazars contributions can be detected with high statistical significance.

dicating that unresolved sources contribute only a modest fraction of the total  $\gamma$ -ray flux (V. S. Paliya et al. 2019).

The right panel of Figure 9 illustrates the trend of the detection significance as a function of the assumed blazars fraction for the HUNT, a  $30 \text{ km}^3$  detector over 3 years, with systematic uncertainties included. When systematic effects are included, the dominant limitation arises from GLF uncertainties. In this case, if blazars contribute to  $\sim 5\%$  of the diffuse neutrino flux above 300 TeV, our method reaches a  $\sqrt{\text{TS}} > 9$  detection significance for 3 years of exposure. For larger assumed fractions, the significance saturates, since the GLF uncertainties impose a systematic floor on the achievable sensitivity. This demonstrates that our approach is capable of identifying even a modest blazar contribution to the diffuse neutrino flux with high confidence.

## 6. CONCLUSIONS

We have evaluated the prospect of diagnosing the correlation between X-ray AGNs and high-energy neutrinos with future neutrino telescopes, incorporating both statistical and systematic effects. By combining a flux-weighted likelihood method with realistic detector performance and observational constraints, we have found that:

- **Dominant role of angular resolution:** The sensitivity of AGN–neutrino correlation is primarily driven by the point-spread function of neutrino detectors. Achieving sub-degree resolution, particularly  $\lesssim 0.1^\circ$ , dramatically reduces background contamination and enhances the significance of de-

tection. For example, with 2000 events and a  $0.1^\circ$  resolution, a  $5\sigma$  detection is achievable, whereas resolutions coarser than  $0.4^\circ$  would require orders of magnitude more events.

- **Source separation criterion:** To minimize source confusion and ensure robust association between neutrinos and AGNs, we require the mean angular separation between two selected AGNs to exceed three times of the detector’s PSF width (i.e.,  $\bar{d} > 3\sigma_{\text{psf}}$ ). This criterion effectively avoids source confusion.
- **Energy threshold optimization:** Increasing the minimum neutrino energy threshold improves the angular resolution and suppresses the atmospheric neutrino background, but at the cost of reducing the event statistics. For a  $30 \text{ km}^3$  undersea/underwater neutrino telescope (e.g., HUNT) that features rapidly improving angular resolution with energy (down to  $\sim 0.04^\circ$  above 300 TeV), the optimal sensitivity is reached at a threshold of a few hundred TeV. In contrast, IceCube-Gen2 shows a weaker energy dependence in its angular resolution; for this detector, selecting  $E_\nu > 100 \text{ TeV}$  strikes a better balance between the angular precision and event statistics.
- **Flux-limited AGN extrapolation and XLF systematics:** Our likelihood analysis is performed on a flux-limited AGN subset selected to satisfy  $\bar{d} > 3\sigma_{\text{psf}}$ , ensuring that source confusion does not bias the inference. The total neu-

trino contribution from the full AGN population is then obtained via extrapolation using the AGN XLF. The associated uncertainty is strongly controlled by the adopted flux threshold  $F_{\min}$ . For  $F_{\min} \leq 10^{-14}$  erg cm $^{-2}$  s $^{-1}$ , the extrapolation uncertainty remains small ( $\leq 10\%$ ), whereas for  $F_{\min} \geq 7 \times 10^{-13}$  erg cm $^{-2}$  s $^{-1}$  the inferred total contribution becomes unreliable, as the correction factor is dominated by uncertainties in the faint-end slope and normalization of the XLF.

- **Implications for next-generation neutrino telescopes:** In the energy range above 300 TeV, a 30 km $^3$ -scale underwater neutrino telescope is expected to reach a significance of  $8.7\sigma$  with one year of exposure. With five years of exposure, the significance increases to  $\sim 19\sigma$ , while the total AGN neutrino fraction can be constrained to a relative precision of  $\delta \simeq 10\%$ . For IceCube-Gen2, considering all neutrinos above 100 TeV, the achievable confidence level is  $\sim 3.1\sigma$  with five years of exposure.
- **Sensitivity to partial AGN contributions:** For a 30 km $^3$ -scale underwater neutrino telescope, if AGNs contribute a fraction  $\alpha \leq 0.17$  of the total diffuse neutrino flux, it is not distinguishable from an isotropic background at the  $3\sigma$  level with

three years of exposure. Even with an extended exposure of 10 years, contribution below  $\alpha \simeq 0.09$  remains undetectable at the same significance. For a larger contribution, the detection significance scales approximately linearly with  $f_{\text{tot}}$ .

These results demonstrate that next-generation neutrino observatories with sub-degree angular precision and sufficient exposure have the potential to confirm or strongly constrain the AGN origin of high-energy neutrinos. Deep multi-wavelength AGN surveys, especially in X-rays, are crucial to minimize uncertainties in the flux extrapolation and to fully exploit the discovery potential of upcoming facilities.

We would like to thank Tian-Qi Huang and Shiqi Yu for valuable discussions. This work is supported by the National Natural Science Foundation of China (grant Nos. 12333006, 12121003 and 12393852), National SKA Program of China (2025SKA0110104) and the Fundamental Research Funds for the Central Universities (KG202502). We are grateful to the High Performance Computing Center of Nanjing University for doing the numerical calculations in this paper on its blade cluster system.

## APPENDIX

### A. BACKGROUND TS DISTRIBUTION AND SIGNIFICANCE CALIBRATION

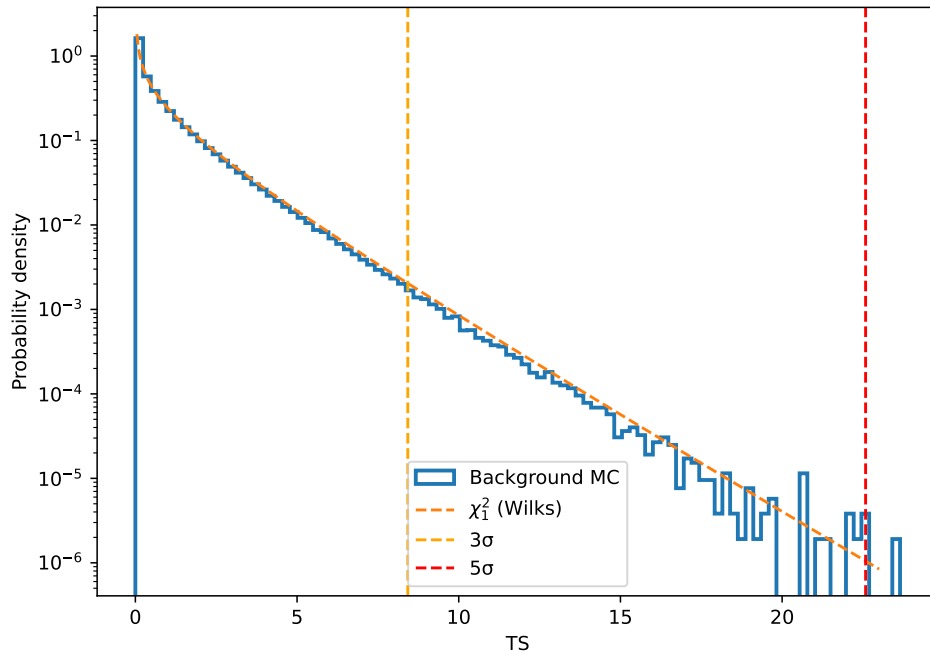
To validate the use of  $\sqrt{\text{TS}}$  as an approximate significance estimator, we generate  $5 \times 10^6$  background-only Monte Carlo realizations for the HUNT detector configuration. For each realization, the test statistic (TS) is computed in the same way as for the observed data.

Figure 10 shows the resulting TS distribution. The empirical distribution is compared to the  $\chi^2$  distribution with one degree of freedom, which represents the theoretical expectation under Wilks' theorem (S. S. Wilks 1938; G. Cowan et al. 2011) for a single free parameter. The vertical dashed lines indicate the TS values corresponding to  $3\sigma$  (orange) and  $5\sigma$  (red) significance levels based on the empirical distribution.

As seen in the figure, the background TS distribution is in good agreement with the Wilks expectation for the TS range of interest, justifying the common approximation of statistical significance as  $\sigma \simeq \sqrt{\text{TS}}$ . Small deviations may occur at very low TS values, but they do not affect the interpretation of the results in the parameter space considered.

## REFERENCES

- |  |  |
|--|--|
| <p>Aartsen, M. G., Abraham, K., Ackermann, M., et al. 2017, The Contribution of Fermi-2LAC Blazars to Diffuse TeV-PeV Neutrino Flux, ApJ, 835, 45, doi: 10.3847/1538-4357/835/1/45</p> | <p>Aartsen, M. G., Ackermann, M., Adams, J., et al. 2020a, Time-Integrated Neutrino Source Searches with 10 Years of IceCube Data, PhRvL, 124, 051103, doi: 10.1103/PhysRevLett.124.051103</p> |
|--|--|



**Figure 10.** Test statistic (TS) distribution obtained from  $5 \times 10^6$  background-only Monte Carlo simulations for the HUNT detector. The histogram shows the empirical TS distribution from simulations. The dashed black line indicates the theoretical expectation from Wilks' theorem for one free parameter ( $\chi_1^2$ ). The vertical dashed orange and red lines indicate the TS thresholds corresponding to  $3\sigma$  and  $5\sigma$  single-tail significance, respectively.

Aartsen, M. G., Ackermann, M., Adams, J., et al. 2020b, Characteristics of the Diffuse Astrophysical Electron and Tau Neutrino Flux with Six Years of IceCube High Energy Cascade Data, *PhRvL*, 125, 121104, doi: [10.1103/PhysRevLett.125.121104](https://doi.org/10.1103/PhysRevLett.125.121104)

Aartsen, M. G., Abbasi, R., Ackermann, M., et al. 2021, IceCube-Gen2: the window to the extreme Universe, *Journal of Physics G Nuclear Physics*, 48, 060501, doi: [10.1088/1361-6471/abbd48](https://doi.org/10.1088/1361-6471/abbd48)

Abbasi, R., Ackermann, M., Adams, J., et al. 2022, Improved Characterization of the Astrophysical Muon-Neutrino Flux with 9.5 Years of IceCube Data, *The Astrophysical Journal*, 928, 50, doi: [10.3847/1538-4357/ac4d29](https://doi.org/10.3847/1538-4357/ac4d29)

Abbasi, R., Ackermann, M., Adams, J., et al. 2022, Search for neutrino emission from cores of active galactic nuclei, *PhRvD*, 106, 022005, doi: [10.1103/PhysRevD.106.022005](https://doi.org/10.1103/PhysRevD.106.022005)

Abbasi, R., Ackermann, M., Adams, J., et al. 2023, Search for Correlations of High-energy Neutrinos Detected in IceCube with Radio-bright AGN and Gamma-Ray Emission from Blazars, *ApJ*, 954, 75, doi: [10.3847/1538-4357/acdfcb](https://doi.org/10.3847/1538-4357/acdfcb)

Abbasi, R., Ackermann, M., Adams, J., et al. 2024, Probing the Connection between IceCube Neutrinos and MOJAVE AGN, *ApJ*, 973, 97, doi: [10.3847/1538-4357/ad643d](https://doi.org/10.3847/1538-4357/ad643d)

Abbasi, R., Ackermann, M., Adams, J., et al. 2025a, Evidence for Neutrino Emission from X-ray Bright Active Galactic Nuclei with IceCube, arXiv e-prints, arXiv:2510.13403, doi: [10.48550/arXiv.2510.13403](https://doi.org/10.48550/arXiv.2510.13403)

Abbasi, R., Ackermann, M., Adams, J., et al. 2025b, Search for Neutrino Emission from Hard X-Ray AGN with IceCube, *ApJ*, 981, 131, doi: [10.3847/1538-4357/ada94b](https://doi.org/10.3847/1538-4357/ada94b)

Acciari, V. A., Ansoldi, S., Antonelli, L. A., et al. 2019, Constraints on Gamma-Ray and Neutrino Emission from NGC 1068 with the MAGIC Telescopes, *ApJ*, 883, 135, doi: [10.3847/1538-4357/ab3a51](https://doi.org/10.3847/1538-4357/ab3a51)

Ackermann, M., Ajello, M., Albert, A., et al. 2015, The Spectrum of Isotropic Diffuse Gamma-Ray Emission between 100 MeV and 820 GeV, *ApJ*, 799, 86, doi: [10.1088/0004-637X/799/1/86](https://doi.org/10.1088/0004-637X/799/1/86)

Ackermann, M., Ajello, M., Albert, A., et al. 2016, Resolving the Extragalactic  $\gamma$ -Ray Background above 50 GeV with the Fermi Large Area Telescope, *PhRvL*, 116, 151105, doi: [10.1103/PhysRevLett.116.151105](https://doi.org/10.1103/PhysRevLett.116.151105)

Adrián-Martínez, S., Ageron, M., Aharonian, F., et al. 2016, Letter of intent for KM3NeT 2.0, *Journal of Physics G Nuclear Physics*, 43, 084001, doi: [10.1088/0954-3899/43/8/084001](https://doi.org/10.1088/0954-3899/43/8/084001)

- Ajello, M., Baldini, L., Ballet, J., et al. 2022, The Fourth Catalog of Active Galactic Nuclei Detected by the Fermi Large Area Telescope: Data Release 3, *ApJS*, 263, 24, doi: [10.3847/1538-4365/ac9523](https://doi.org/10.3847/1538-4365/ac9523)
- Ambrosone, A. 2024, Berezinsky Hidden Sources: An Emergent Tension in the High-Energy Neutrino Sky? arXiv, doi: [10.48550/ARXIV.2406.13336](https://doi.org/10.48550/ARXIV.2406.13336)
- Ballet, J., Bruel, P., Burnett, T. H., Lott, B., & The Fermi-LAT collaboration. 2023, Fermi Large Area Telescope Fourth Source Catalog Data Release 4 (4FGL-DR4), arXiv e-prints, arXiv:2307.12546, doi: [10.48550/arXiv.2307.12546](https://doi.org/10.48550/arXiv.2307.12546)
- Barcons, X. 1992, Confusion Noise and Source Clustering, *ApJ*, 396, 460, doi: [10.1086/171733](https://doi.org/10.1086/171733)
- Bechtol, K., Ahlers, M., Di Mauro, M., Ajello, M., & Vandenbroucke, J. 2017, Evidence against Star-forming Galaxies as the Dominant Source of Icecube Neutrinos, *ApJ*, 836, 47, doi: [10.3847/1538-4357/836/1/47](https://doi.org/10.3847/1538-4357/836/1/47)
- Belolaptikov, I., Dzhilkibaev, Z. A. M., Allakhverdyan, V. A., et al. 2022, in 37th International Cosmic Ray Conference, 2, doi: [10.22323/1.395.002](https://doi.org/10.22323/1.395.002)
- Bradascio, F., & Glüsenkamp, T. 2019, in European Physical Journal Web of Conferences, Vol. 207, European Physical Journal Web of Conferences (EDP), 05002, doi: [10.1051/epjconf/201920705002](https://doi.org/10.1051/epjconf/201920705002)
- Braun, J., Dumm, J., De Palma, F., et al. 2008, Methods for Point Source Analysis in High Energy Neutrino Telescopes, *Astroparticle Physics*, 29, 299, doi: [10.1016/j.astropartphys.2008.02.007](https://doi.org/10.1016/j.astropartphys.2008.02.007)
- Brunner, H., Liu, T., Lamer, G., et al. 2022, The eROSITA Final Equatorial Depth Survey (eFEDS). X-ray catalogue, *A&A*, 661, A1, doi: [10.1051/0004-6361/202141266](https://doi.org/10.1051/0004-6361/202141266)
- Buson, S., Tramacere, A., Pfeiffer, L., et al. 2022, Beginning a Journey Across the Universe: The Discovery of Extragalactic Neutrino Factories, *ApJL*, 933, L43, doi: [10.3847/2041-8213/ac7d5b](https://doi.org/10.3847/2041-8213/ac7d5b)
- Capanema, A., Esmaili, A., & Murase, K. 2020, New constraints on the origin of medium-energy neutrinos observed by IceCube, *PhRvD*, 101, 103012, doi: [10.1103/PhysRevD.101.103012](https://doi.org/10.1103/PhysRevD.101.103012)
- Cowan, G., Cranmer, K., Gross, E., & Vitells, O. 2011, Asymptotic formulae for likelihood-based tests of new physics, *European Physical Journal C*, 71, 1554, doi: [10.1140/epjc/s10052-011-1554-0](https://doi.org/10.1140/epjc/s10052-011-1554-0)
- Creque-Sarbinowski, C., Kamionkowski, M., & Zhou, B. 2022, Seeking Neutrino Emission from AGN through Temporal and Spatial Cross-Correlation, *Physical Review D*, 105, 123035, doi: [10.1103/PhysRevD.105.123035](https://doi.org/10.1103/PhysRevD.105.123035)
- Das, S., Razzaque, S., & Gupta, N. 2022, Cosmogenic gamma-ray and neutrino fluxes from blazars associated with IceCube events, *A&A*, 658, L6, doi: [10.1051/0004-6361/202142123](https://doi.org/10.1051/0004-6361/202142123)
- Eichmann, B., Oikonomou, F., Salvatore, S., Dettmar, R.-J., & Tjus, J. B. 2022, Solving the Multimessenger Puzzle of the AGN-starburst Composite Galaxy NGC 1068, *ApJ*, 939, 43, doi: [10.3847/1538-4357/ac9588](https://doi.org/10.3847/1538-4357/ac9588)
- Fang, K., Gallagher, J. S., & Halzen, F. 2022, The TeV Diffuse Cosmic Neutrino Spectrum and the Nature of Astrophysical Neutrino Sources, *ApJ*, 933, 190, doi: [10.3847/1538-4357/ac7649](https://doi.org/10.3847/1538-4357/ac7649)
- Fiorillo, D. F. G., Comisso, L., Peretti, E., Petropoulou, M., & Sironi, L. 2025, The contribution of turbulent AGN coronae to the diffuse neutrino flux, arXiv e-prints, arXiv:2504.06336, doi: [10.48550/arXiv.2504.06336](https://doi.org/10.48550/arXiv.2504.06336)
- Huang, T. Q., Cao, Z., Chen, M., et al. 2024, in 38th International Cosmic Ray Conference, 1080
- Huang, T. Q., & HUNT Collaboration. 2025, in 39th International Cosmic Ray Conference, 1061
- IceCube Collaboration, Aartsen, M. G., Ackermann, M., et al. 2018, Neutrino emission from the direction of the blazar TXS 0506+056 prior to the IceCube-170922A alert, *Science*, 361, 147, doi: [10.1126/science.aat2890](https://doi.org/10.1126/science.aat2890)
- IceCube Collaboration, Abbasi, R., Ackermann, M., et al. 2022, Evidence for neutrino emission from the nearby active galaxy NGC 1068, *Science*, 378, 538, doi: [10.1126/science.abg3395](https://doi.org/10.1126/science.abg3395)
- Inoue, Y., Khangulyan, D., & Doi, A. 2020, On the Origin of High-energy Neutrinos from NGC 1068: The Role of Nonthermal Coronal Activity, *ApJL*, 891, L33, doi: [10.3847/2041-8213/ab7661](https://doi.org/10.3847/2041-8213/ab7661)
- Jones, M. G., Haynes, M. P., Giovanelli, R., & Papastergis, E. 2016, When is stacking confusing? The impact of confusion on stacking in deep H I galaxy surveys, *MNRAS*, 455, 1574, doi: [10.1093/mnras/stv2394](https://doi.org/10.1093/mnras/stv2394)
- Kheirandish, A., Murase, K., & Kimura, S. S. 2021, High-energy Neutrinos from Magnetized Coronae of Active Galactic Nuclei and Prospects for Identification of Seyfert Galaxies and Quasars in Neutrino Telescopes, *ApJ*, 922, 45, doi: [10.3847/1538-4357/ac1c77](https://doi.org/10.3847/1538-4357/ac1c77)
- Kowalski, M., Ackermann, M., & Bartos, I. 2025, The promise of deep-stacking for neutrino astronomy, arXiv e-prints, arXiv:2501.10213, doi: [10.48550/arXiv.2501.10213](https://doi.org/10.48550/arXiv.2501.10213)
- Kun, E., Bartos, I., Tjus, J. B., et al. 2024, Possible correlation between unabsorbed hard x rays and neutrinos in radio-loud and radio-quiet active galactic nuclei, *PhRvD*, 110, 123014, doi: [10.1103/PhysRevD.110.123014](https://doi.org/10.1103/PhysRevD.110.123014)

- Kurczynski, P., & Gawiser, E. 2010, A Simultaneous Stacking and Deblending Algorithm for Astronomical Images, *AJ*, 139, 1592, doi: [10.1088/0004-6256/139/4/1592](https://doi.org/10.1088/0004-6256/139/4/1592)
- Liu, T., Buchner, J., Nandra, K., et al. 2022, The eROSITA Final Equatorial-Depth Survey (eFEDS): The AGN Catalog and Its X-ray Spectral Properties, *Astronomy & Astrophysics*, 661, A5, doi: [10.1051/0004-6361/202141643](https://doi.org/10.1051/0004-6361/202141643)
- Manconi, S., Korsmeier, M., Donato, F., et al. 2020, Testing gamma-ray models of blazars in the extragalactic sky, *PhRvD*, 101, 103026, doi: [10.1103/PhysRevD.101.103026](https://doi.org/10.1103/PhysRevD.101.103026)
- Miller, K. A., & Stone, J. M. 2000, The Formation and Structure of a Strongly Magnetized Corona above a Weakly Magnetized Accretion Disk, *ApJ*, 534, 398, doi: [10.1086/308736](https://doi.org/10.1086/308736)
- Murase, K., Guetta, D., & Ahlers, M. 2016, Hidden Cosmic-Ray Accelerators as an Origin of TeV-PeV Cosmic Neutrinos, *PhRvL*, 116, 071101, doi: [10.1103/PhysRevLett.116.071101](https://doi.org/10.1103/PhysRevLett.116.071101)
- Murase, K., Inoue, Y., & Dermer, C. D. 2014, Diffuse neutrino intensity from the inner jets of active galactic nuclei: Impacts of external photon fields and the blazar sequence, *PhRvD*, 90, 023007, doi: [10.1103/PhysRevD.90.023007](https://doi.org/10.1103/PhysRevD.90.023007)
- Murase, K., Kimura, S. S., & Mészáros, P. 2020, Hidden Cores of Active Galactic Nuclei as the Origin of Medium-Energy Neutrinos: Critical Tests with the MeV Gamma-Ray Connection, *PhRvL*, 125, 011101, doi: [10.1103/PhysRevLett.125.011101](https://doi.org/10.1103/PhysRevLett.125.011101)
- Paliya, V. S., Domínguez, A., Ajello, M., Franckowiak, A., & Hartmann, D. 2019, Fermi-LAT Stacking Analysis Technique: An Application to Extreme Blazars and Prospects for their CTA Detection, *ApJL*, 882, L3, doi: [10.3847/2041-8213/ab398a](https://doi.org/10.3847/2041-8213/ab398a)
- Salvato, M., Wolf, J., Dwelly, T., et al. 2025, Counterpart identification and classification for eRASS1 and characterisation of the active galactic nuclei content, *A&A*, 704, A344, doi: [10.1051/0004-6361/202556142](https://doi.org/10.1051/0004-6361/202556142)
- Saurenhaus, L., Capel, F., Oikonomou, F., & Buchner, J. 2025, Constraining the contribution of Seyfert galaxies to the diffuse neutrino flux in light of point source observations, arXiv e-prints, arXiv:2507.06110, doi: [10.48550/arXiv.2507.06110](https://doi.org/10.48550/arXiv.2507.06110)
- Senno, N., Mészáros, P., Murase, K., Baerwald, P., & Rees, M. J. 2015, Extragalactic Star-forming Galaxies with Hypernovae and Supernovae as High-energy Neutrino and Gamma-ray Sources: the case of the 10 TeV Neutrino data, *ApJ*, 806, 24, doi: [10.1088/0004-637X/806/1/24](https://doi.org/10.1088/0004-637X/806/1/24)
- Ueda, Y., Akiyama, M., Hasinger, G., Miyaji, T., & Watson, M. G. 2014, TOWARD THE STANDARD POPULATION SYNTHESIS MODEL OF THE X-RAY BACKGROUND: EVOLUTION OF X-RAY LUMINOSITY AND ABSORPTION FUNCTIONS OF ACTIVE GALACTIC NUCLEI INCLUDING COMPTON-THICK POPULATIONS, *The Astrophysical Journal*, 786, 104, doi: [10.1088/0004-637X/786/2/104](https://doi.org/10.1088/0004-637X/786/2/104)
- Wilks, S. S. 1938, The large-sample distribution of the likelihood ratio for testing composite hypotheses, *Annals of Mathematical Statistics*, 9, 60, doi: [10.1214/aoms/1177732360](https://doi.org/10.1214/aoms/1177732360)
- Willox, E., & HAWC Collaboration. 2022, HAWC Follow-up on IceCube evidence from NGC 1068, *The Astronomer's Telegram*, 15765, 1
- Ye, Z. P., Hu, F., Tian, W., et al. 2023, A multi-cubic-kilometre neutrino telescope in the western Pacific Ocean, *Nature Astronomy*, 7, 1497, doi: [10.1038/s41550-023-02087-6](https://doi.org/10.1038/s41550-023-02087-6)
- Zegarelli, A., Franckowiak, A., Sommani, G., Valtonen-Mattila, N., & Yuan, T. 2025, IceCat-2: Updated IceCube Event Catalog of Alert Tracks, arXiv e-prints, arXiv:2507.06176, doi: [10.48550/arXiv.2507.06176](https://doi.org/10.48550/arXiv.2507.06176)
- Zhang, H., Cui, Y., Huang, Y., et al. 2025, A Proposed Deep Sea Neutrino Observatory in the Nanhai, *Astroparticle Physics*, 171, 103123, doi: [10.1016/j.astropartphys.2025.103123](https://doi.org/10.1016/j.astropartphys.2025.103123)
- Zhou, B., Kamionkowski, M., & Liang, Y.-f. 2021, Search for high-energy neutrino emission from radio-bright AGN, *PhRvD*, 103, 123018, doi: [10.1103/PhysRevD.103.123018](https://doi.org/10.1103/PhysRevD.103.123018)